On the development and evolution of wear flats in microcrystalline sintered alumina grinding wheels

L.Godino[(1)], I.Pombo[(2)], J.A.Sanchez[(2)] J.Alvarez[(3)]

[(1)] Faculty of Engineering Bilbao, University of the Basque Country (UPV/EHU), Plaza Torres Quevedo, 1, 48013 Bilbao (Spain) leire.godino@ehu.eus

[(2)] Faculty of Engineering Bilbao, University of the Basque Country (UPV/EHU), Plaza Torres Quevedo, 1, 48013 Bilbao (Spain)

[(3)] IK4-Ideko, Arriaga Kalea, 2, 20870 Elgoibar, Gipuzkoa, Spain

Abstract

Wheel wear is a critical issue for grinding process optimization. This is why it receives so much attention both from Academia and industry. The development of new generations of abrasive wheels requires improving the understanding of the mechanisms involved in the loss of abrasive capacity of the wheels. In the case of alumina wheels, which are largely used in many grinding operations, the development of microcrystalline sintered alumina grains is one of the most important innovations to emerge since the early 1980's. In comparison with white fused alumina this grains are characterized by higher ductility and have approximately 5 % more hardness. However, the mechanisms of occurrence of wear flats in these new abrasives are still to be fully understood. In this work, a novel approach to the study of the underlying phenomena that occur during the development of wear flats in microcrystalline sintered alumina grains is presented. Experimental results in terms of grinding forces, friction coefficient and surface analysis are presented and compared to those obtained with conventional white fused alumina. The value of wear flat area is as much as 25 % higher in the case of microcrystalline sintered alumina grains. Results will be useful to prevent the development of grinding burns resulting from wear flat development in these new alumina wheels.

Keywords

Grinding, wheel, Wear-flat

Abbreviations

a_e	[µm]	Depth of cut
a_d	[µm]	Dressing depth
%A	[-]	Percentage of area corresponding to wear flat
b	[mm]	Grinding width
Q_w'	[$mm^3/mm \cdot s$]	Specific removal rate
q_s	[-]	Speed ratio v_w/v_s
SG	[-]	Sintered Sol Gel Alumina
S_k	[µm]	Core roughness depth
S_{pk}	[µm]	Reduced peak height
S_{vk}	[µm]	Reduced valley depth
v_d	[mm/min]	Dresser speed
v_s	[m/s]	Wheel speed
v_w	[mm/min]	Workpiece speed
V'_w	[mm^3/mm]	Specific material removal
WFA	[-]	White Fused Alumina

1. Introduction

The grinding process is constantly adapting to new requirements in the industry, with particular attention being paid to the production of high quality surfaces whilst increasing process efficiency. One of the handicaps of grinding and machining processes in general is the low machinability of new materials. Moreover, from an industrial point of view, higher removal rates are demanded and an increased life of the grinding wheels is required to enhance the production process. In order to meet these objectives, new developments are required for both the grinding process and the grinding wheels [1], [2], [3].

With regard to improvements in grinding wheels, the creation and development of microcrystalline sintered alumina grains is one of the most important innovations to emerge since the early 1980's. This type of alumina is denoted by the trade names of SG™, TG™ or Cubitron™, among others. Approximately 30 years ago, this new generation of microcrystalline sintered Al_2O_3 began to be studied by the 3M company and years later SG™ was patented by Norton [4].

SG grains, in comparison with white fused alumina (WFA), are characterized by higher ductility and have approximately 5 % more hardness [5], [6], which improves the resistance to brittle fracture. However, the shape is similar, with the main difference being the number and size of crystals. WFA is composed of 3 or 4 crystals while SG grains is made from thousands of micro-crystals, randomly oriented and usually between 0.1 and 5 µm in size

[4]. Such a structure facilitates microfracture, leading to the self-sharpening phenomenon of SG grains [5], [6].

In terms of service life, SG grains are more durable than WFA — between 5 and 30 times more — with up to 10 times greater machining efficiency [4]. In general, SG abrasives are used for applications that require a high removal rate. The main objective is to optimize productivity and to reduce the cost of the process. Applications of these wheels include tool steels (AISI D2), bearing ring steels (100Cr6) and superalloys [7].

The use of this kind of abrasive is currently common in industry. However, a deeper insight into the fundamental mechanisms such as wear behaviour or heat conduction must be gained for optimum application of these abrasives [8], [9]. This lack of knowledge limits the optimum design of the grinding process using these types of wheels.

To provide an exhaustive characterization of grinding wheel wear, it is firstly important to distinguish between the wear mechanisms of abrasive grains and types of grinding wheel wear. On the one hand, abrasive grains are subject to different wear mechanisms, including chipping, abrasive wear, plastic deformation, and chemical reactions, among others [5], [6], [10]. All of these overlap during contact between abrasive grains and workpiece material, and hence it is difficult to study each mechanism separately during the process.

On the other hand, the main types of wear are grain fracture, bond fracture and wear flat [5], [6], [10]. One of these will be predominant depending on the structure of the grinding wheel, the nature of the abrasive grains, and even the grinding conditions, which change the force applied on the grains. Each of the wear types mentioned presents consequences for the final result of the process. For the case of grain or bond fracture, volumetric wear will be predominant, involving shape errors or dimensional deviations in the workpiece [6]. In contrast, wear flat results in an increase of power and specific energy during the process, thermal damage and loss of accuracy in the workpiece, implying significant economic losses in production [4]. This kind of wear modifies contact conditions during the process. Studies have shown the increase in the real contact area and hence the normal force during grinding, together with variations in the friction coefficient [11], [12].

Consequently, from a scientific point of view, the study of the appearance of wear flat in the surface of grinding wheels is key to understanding their behaviour during the grinding process. Wear flat is wear of a tribochemical nature [10]. Various phenomena occur simultaneously such as mechanical friction, plastic flow of abrasives at high temperatures, crumbling and chemical reactions between the workpiece material and the abrasive [2]. Depending on the materials in contact, chemical reactions acquire great importance, fuelled by the high temperatures reached. Contact conditions determine wear flat generation, usually quantified in terms of the percentage of flat surface compared with the apparent area of the grinding wheel surface, which is usually referred to as the wear flat area *A%*.

From a tribological point of view, ceramic-metal contact has long been analysed and used for a wide variety of applications, such as hip prosthesis or ceramic bearings. The work of Ravikiran is noteworthy due to an abundance of studies analysing the tribological contact of alumina and steel [13]–[15]. These works characterize the behaviour of zirconia-toughened alumina (ZTA) or 87 % Al_2O_3 alumina under different contact conditions. Maximum values of sliding speed and pressure reached on pin on disk tribometer are 12 m/s and 50 MPa respectively. Analysing the wear of Al_2O_3, a third body, is formed due to chemical

interactions that occur on contact. This third body is composed of materials in contact and could either be deposited on both bodies in contact or remain between the two bodies. This layer changes contact conditions, affecting the friction coefficient [14]. The contact conditions achieved in Ravikiran's work are far removed from those achieved in contact during the grinding process — approximately 35 m/s and 1-2 GPa. Nonetheless, these results represent the first step towards understanding wear behaviour during grinding.

Similarly, Klocke has characterized SG alumina on pin on disk tribometer at a very low sliding speed of 2 m/s and a high pressure, from 0.5 to 1.5 GPa [16]. Due to the high pressure and continued contact, high local temperatures are achieved. Analysing wear alumina, the third body is generated and adheres to plastically deformed SG alumina. This layer is mainly composed of FeO, with spinel ($FeAl_2O_4$) inlays attached both to the oxide layer and to deformed SG alumina.

However, in the pin on disk test, the thermal cycles suffered by abrasive grains during grinding are not adequately reproduced. Whilst in the pin on disk test the contact between the alumina and steel is continuous, during grinding the contact is intermittent. The temperature reached in both cases could be different and alumina wear during grinding and on pin on disk tribometer could change. Thus, an, in-process analysis is required.

With regard to the grinding process, the first studies related to grinding wheel wear were carried out by Malkin [11], [12], [17]. These studies involve not only wear flat but also fracture wear, analysing the influence on process parameters and the mechanism that leads to wear. These studies used monocrystal alumina wheels during surface grinding. Experimental results revealed that the percentage of wear flat area increases with wheel hardness. Consequently, a harder grinding wheel implies a higher normal and tangential force and a lower force ratio. These differences are amplified if fine dressing is carried out as opposed to coarse dressing [11]. In this study, in which steel and alumina were the material in contact, spinel ($FeAl_2O_4$) was the predominant component of the third body [10]. The main challenge of evaluating wear fat during grinding is the difficulty in isolating this type of wear.

More recent experimental works related to grinding have been carried out by Nadolny, characterizing the wear of SG alumina during internal cylindrical grinding [7]. This work is concerned with wheel life, wheel topography, and the most predominant wear phenomena. This characterization was conducted for different SG wheels varying in terms of vitrified bond. Nadolny established that in the contact area of SG grains, there is a combined effect of abrasive wear, plastic flow, thermo-fatigue wear, and micro chipping. For a high percentage of bonding, abrasive wear and plastic flow of alumina are the main wear phenomena, leading to wear flat in SG wheels. His work also confirmed that plastic deformations occur due to the sliding and subsequent adhesion of microcrystals. Both the size of the microcrystals and strain level influence the plastic deformation of SG alumina [7]. Nadolny´s work focused on the behaviour of SG wheels during grinding, rather than a thorough analysis in terms of microscopic behaviour. Furthermore, different types of wear occur simultaneously, without isolating each of the phenomena. The advantage of this work is that it was conducted under real grinding conditions, and, as Klocke concluded from the results of the pin on disk test, plastic deformation of SG abrasive grains takes place under these conditions.

Focusing on the third body, it was found in both Malkin's and Klocke's works that it is adhered to alumina. However, the main composition is different even though in both cases Al_2O_3 was used. $FeAl_2O_4$ was found to adhere to monocrystal grains whilst FeO adhered to SG grains. The difference in the temperature reached during contact results in different chemical reactions. The composition of the third body depends on the materials in contact, the temperature reached in the contact areas, as well as the pressure and sliding speed values obtained during contact [18].

Furthermore, Klocke established that the thermal conductivity of WFA is higher than that of SG [16]. This difference is revealed mainly due to the great quantity of boundaries that SG alumina presents, in contrast to WFA alumina. These imperfections lead to lower conductivity, and hence the SG alumina reaches higher temperatures in contact.

This work primarily focuses on analysing the appearance of wear flat in abrasive grains during grinding. As previously mentioned, the appearance of wear flat is the main factor responsible for the increase of power consumption during the process and the occurrence of thermal damage in the ground part. It is important to note that a complete study of the wear in grinding wheels should be much more extensive and has only been partially developed by other authors such as Malkin [12] or Nadolny [8]. Therefore the aim of this work is to build on these initial conclusions and hypotheses regarding the appearance of wear flat and to examine the influence of crystallographic structure, taking into account the most recent advances in this field.

Taking all these facts into account, the current paper presents a novel approach to the study of the underlying phenomena that occur during the development of wear flat in alumina grinding wheels. To this end, an experimental methodology was devised to isolate the wear flat effect from other types of wear, whilst reproducing the contact conditions typical of real-life grinding operations. This methodology is described in Section 2. The grinding experiments — listed in Section 3 — were designed in which an extremely hard grinding wheel was employed so that the development of wear flats emerges as the predominant effect. Experimental tests were implemented on both the WFA and SG grinding wheel, comparing the development of wear flat and its effect on process parameters. Moreover the influence of the type of abrasive, depth of cut, and workpiece speed was manipulated to analyse their effects, maintaining constant wheel speed. A discussion of the results in terms of forces, friction coefficient, and surface analysis is presented in Section 4.

The main results show that due to the lower thermal conductivity of SG alumina in comparison with WFA, the value of $\%A$ is 23 % higher for SG than WFA. Consequently, SG develops a very homogeneous appearance with a higher quantity of third body adhered to flat grains, maintaining a friction coefficient value of 0.35. The results will be useful for better understanding the development of wear flat and its impact on both process parameters and round surface. Knowledge of evolution of wear flat is critical to prevent grinding burns.

2. Methodology and experimental set up

To avoid grain pull out and breakage, and therefore to isolate wear flat, it was proposed to use an extremely hard (high grade) grinding wheel (see Table 1). Further, to observe wear flat in more detail, a close structure grinding wheel was chosen for both SG and WFA. With

this wheel, tests can be conducted on a universal surface grinder under different grinding conditions (see Table 2), but always within the range of industrial parameters. In addition to the wheel configuration, workpiece material is also of importance. The combination of hard wheels and hard steel promotes the appearance of wear flat on the grinding wheel surface.

Table 1: Set up of the grinding tests and surface analysis.

Surface grinding machine	Blohm Orbit CNC 36
Wheel specification	60R6V89
Wheel dimensions	220x40x127mm
Workpiece Material	Tempered AISI D2 60±2 HRC
Workpiece Dimensions	30x100x20mm
Grinding fluid	Coolant lubricant 5 % oil in water
Grinding fluid flow rate, Q	45 l/min
Dynamometric Device	Kistler 9257B
Microscopes	Optical PCE MM200: Magnification of 60x - 200x Confocal microscope: Objective magnification 10x/0.3 SEM: Magnification of 50 and 500 and EDXA analysis

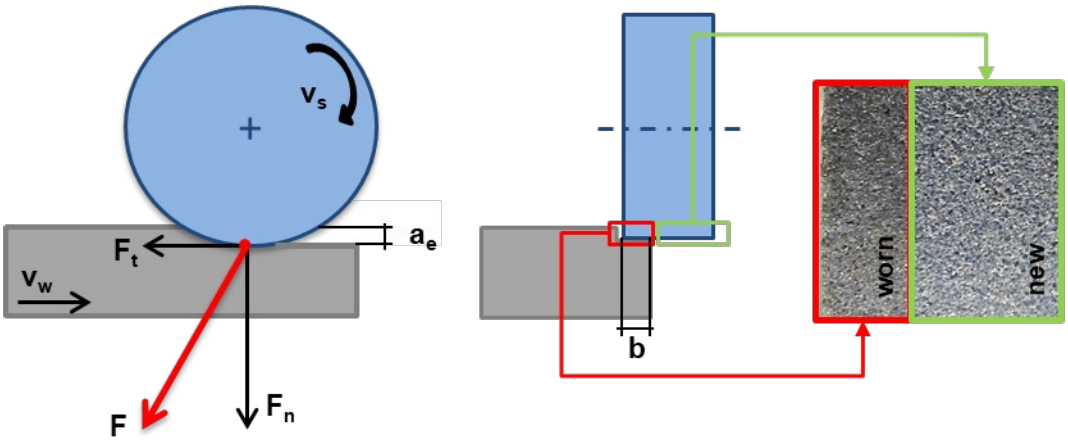

Figure 1: Experimental test scheme and grinding kinematic

The current study employed 4 tests. The scheme of tests and grinding kinematic are shown in Figure 1. Accumulative grinding tests were carried out to analyse the evolution of wear flat. Therefore, during a complete test, only the grinding wheel is dressed before starting the test, in order to have information regarding the initial surface. Experimental tests were conducted with *b*=10 mm, allowing for a real depth of cut measurement and verifying that wheel volumetric wear is negligible and that wear flat is the main source of wear. Grinding forces were also measured during a complete test. On each test 100 mm^3/mm of workpiece

material was removed and images of the surface were taken, each measuring 10 mm^3/mm. The wear test methodology is summarized in Figure 2 (a).

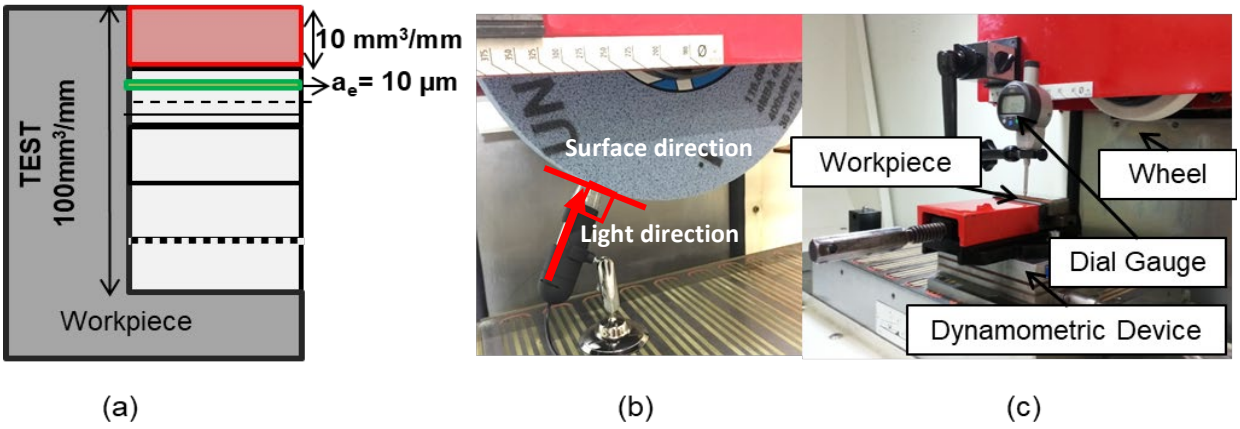

Figure 2: (a) Grinding test methodology, in which a complete test, blocks of 10 mm^3/mm and a_e can be distinguished. (b) Wear flat measurement set up. (c) Experimental test set up.

Characterization of wear flat was carried out by analysing images taken during the test using an optical microscope at magnification of 200. The field of view at this magnification is 2.5 mm x 1.9 mm and the resolution is of 1600x1200 (2.8 µm/pixel). Figure 2 (b) displays the wheel surface measurement set up. To take the images, the coaxial light technique was chosen [20], [21]. Reflected light corresponds to wear flats, and shows whether adhesion of the third body is present or not. These images were then processed on Leica commercial software, which is based on binary segmentation. The images were treated through the implementation of two filters. The purpose of the first filter is to avoid brightness that does not correspond to wear flat areas. This filter deletes areas smaller than a set of 8 pixels, which are considered to have a brightness that is due to the light reflection on surfaces that are not flat. Areas of 8 pixels corresponding to 62.72 μm^2 are negligible comparing with abrasive grain size. The second filter fills in the gaps inside one area due to measurement or brightness identification errors, that is, it adds a pixel to the wear flat area if all pixels around it correspond to a wear flat area. The value of the wear flat area is obtained and represented by *%A*."

To enhance the study of the surface analysis, it is worth analysing the wheel surface topography of just dressed (from now on new) and worn wheel (referring to the state at which 100 mm^3/mm has been removed) using confocal microscope and SEM at high magnification. Surface topography is measured and 3D parameters are achieved using a confocal microscope, and the SEM images complement the surface study, which allow for comparing worn and new abrasive grains and distinguishing third body deposition zones, amongst other phenomena. The differences between new and worn surfaces were also analysed in order to observe the effect of wear flat. Finally, EDXA analysis was applied to the worn wheel. The goal of this analysis was to evaluate materials constituting the third body attached to the flat grains. EDXA analysis also permits identification of the material on the flat surface, which can be abrasive material, bond material, or the third body. These two methods were applied with the aim of better understanding of tribochemical wear that is suffered by the wheel surface during grinding.

Industrial grinding parameters were chosen to carry out the wear tests. Table 2 and Table 3 list the grinding parameters for all tests and the dressing parameters for initial surface suitability. Table 2 also displays the real values of depth of cut and specific removal rate. The variation of workpiece speed and depth of cut allows for studying the influence of cutting parameters on the generation of wear flat. The selected values of depth of cut are appropriate due to the use of an extremely hard wheel. In addition, dressing parameters are chosen to promote wear flat appearance on the wheel surface, with small a_d.

Table 2: Grinding test parameters

Test	v_s [m/s]	v_w [mm/min]	a_e Prog. [µm]	Q_w' Prog. [mm^3/mm·s]	a_e Real [µm]	Q_w' Real [mm^3/mm·s]	q_s
1	30	15000	10	2.5	3	0.75	120
2	30	15000	15	3.8	5	1.25	120
3	30	25000	10	4.2	3	1.25	72
4	30	25000	15	6.3	4	1.67	72

Table 3 Dressing parameters

v_s [m/s]	v_d [mm/min]	a_d [µm]
30	250	10

However, before turning to a discussion about the influence of grinding parameters, it is of interest to justify the differences achieved between programmed and real depth of cut. The values of programmed cutting parameters correspond to a specific removal rate, between 2.5 and 6.3 mm^3/mms. However, the specific removal rates achieved decrease by around 70 % in relation to the programmed rates. The reason for this behavior is likely to be found in the elastic deflection suffered by the machine spindle during grinding. This effect is widely known in the grinding process and in this case it is favored by the considerable hardness of the grinding wheel and the characteristics of the tests.

.

3. Results and discussion

Firstly, the influence of grinding parameters on the development of wear flat is discussed. For both types of abrasive grains, an analysis is presented regarding wear flat evolution with specific material removed, the influence of wear flat on grinding forces, and the friction coefficient. Finally, an in-depth evaluation of wheel topography is presented.

3.1. Grinding analysis

Figure 3 plots the evolution of wear flat with specific removal rate. The effect of both crystallographic structure and grinding parameters are clearly observable on each of the three graphs. Nonetheless, in all the cases studied here an almost linear trend of wear flat growth can be seen, which is entirely compatible with the results obtained by Malkin [11]. With respect to the initial value of *%A*, on each test this value was observed to be around 6 % for the first measurement at 10 mm^3/mm. This relatively high value in comparison with previous studies (which report values of around 2-3 %), could be explained primarily in terms of the stringent conditions used to promote wear flat. The closed structure of the grinding wheel, together with the fine dressing parameters described in Section 2, leads to a smooth surface. Therefore, the initial surface presents flat grains due to the dressing and in the initial phase of testing the most sharpened grains lose their cutting ability. This fact is in accord with the typical wear pattern of cutting tools, presenting rapid wear at the beginning of the tool life. In only 10 mm^3/mm of specific removed material, the *%A* value was already as high as 6 %.

Regarding the influence of the crystalline structure, on Figure 3 (a), higher values of *%A* were found for SG alumina than for WFA. For instance, on Test 2, maintaining constant grinding parameters, v_w=150000 mm/min and a_e=5 µm, the maximum *%A* for WFA is 11 % whilst for SG alumina this value is approximately 14 %. Therefore the microcrystalline structure of SG alumina presents a greater tendency to become flat than WFA when other kinds of abrasive wear are isolated.

These results are also in accord with the work of Klocke et al. [16]. In this study the authors pointed out that the thermal conductivity of the SG abrasive grains was smaller than that of WFA grains due to the greater amount of crystal edges in the first case. This fact is extremely important in the generation of wear flat because having smaller heat conductivity necessarily implies that the temperatures in the grain-workpiece contact will be higher in SG grains than in the case of WFA grains. Given the fact that the generation of wear flat is a tribochemical issue, the higher temperature will facilitate the appearance of wear flat. In addition, low values of a_e generate forces that are not sufficiently strong to produce breakage of microcrystals and avoid the shelf-sharpening of the wheel [6]. According to the results obtained by other researchers in previous studies [16], [21], it can be concluded that, due mainly to the rubbing phase in the grinding process, SG alumina presents a higher tendency to develop wear flat than WFA.

With respect to the influence of grinding parameters, the effect of both real depth of cut and workpiece speed can be distinguished. If wear flat appearance comparison is done maintaining v_w constant Figure *3* (b), generated wear flat increase with depth of cut. In the particular case of SG alumina and v_w=15000 mm/min, wear flat increases from 6 % to 10 % for a_e=3 µm and from 6 % to 13 % for a_e=5 µm. Therefore, an increase of 23 % of wear flat at the end of the tests is observed with an increase of a_e from 3 µm to 5 µm. However, this correlation between *%A* and a_e will only occur when the grinding forces are lower than the retaining forces of the grains. The high hardness of the grinding wheel (R) and small real depth of cut implies that in the present study the correlation of %A and a_e is valid. For other cases in which grinding forces are higher than retaining forces, when using, for instance, a very soft grinding wheel, grain pull out will be the predominant source of wear, and the *% A* measured would decrease with a_e*".*

Finally, Figure *3* (c) shows the influence of v_w for SG alumina when maintaining constant a_e=3 µm. Although the differences in maximum values of *%A* are negligible, there are differences in the trends of both speeds. The pattern of wear flat evolution presents a higher slope for the higher workpiece speed.

The maximum values of *%A* found in this work, 13 %, are significantly higher than those reported in the study by Malkin [11], where values of approximately 6 % were found in both cases for 100 mm^3/mm. However, this difference can primarily be explained primarily in terms of the grinding wheel hardness and the aim to promote wear flat in the current study. Nonetheless, the results presented here are in agreement with the findings confirmed in the study by Malkin, verifying that the presence of wear flat increases with greater wheel hardness.

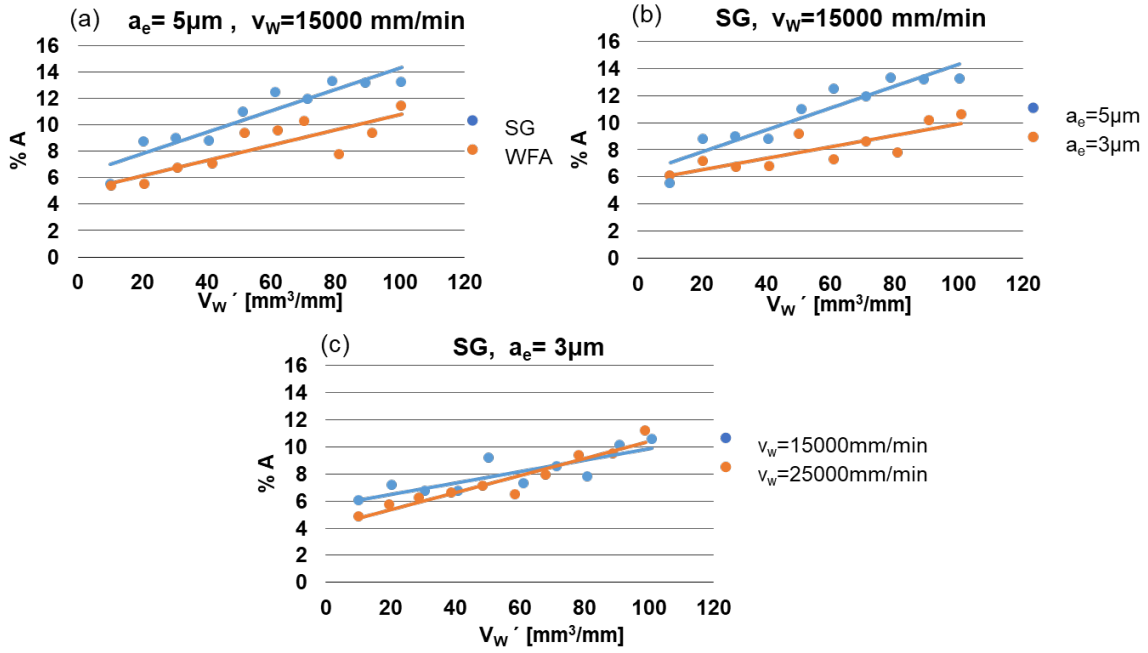

Figure 3: Wear flat evolution with specific removal rate. (a) Crystallographic structure variation. (b) Depth of cut variation. (c) Workpiece speed variation

In relation to the forces involved in the process, Figure 4 plots the results from Test 2, a_e=5 µm and v_w=15000 mm/min, for both SG and WFA abrasive grains. Hereafter, the results presented from Test 2 are representative of each of the tests carried out. Thus, given force for WFA and SG show the same evolution and similar values. Both normal and tangential force-directions present a very slight increase as the grinding wheel is worn, reaching a value of around 22 N/mm for normal specific force-direction and around 8 N/mm for tangential specific force-direction.

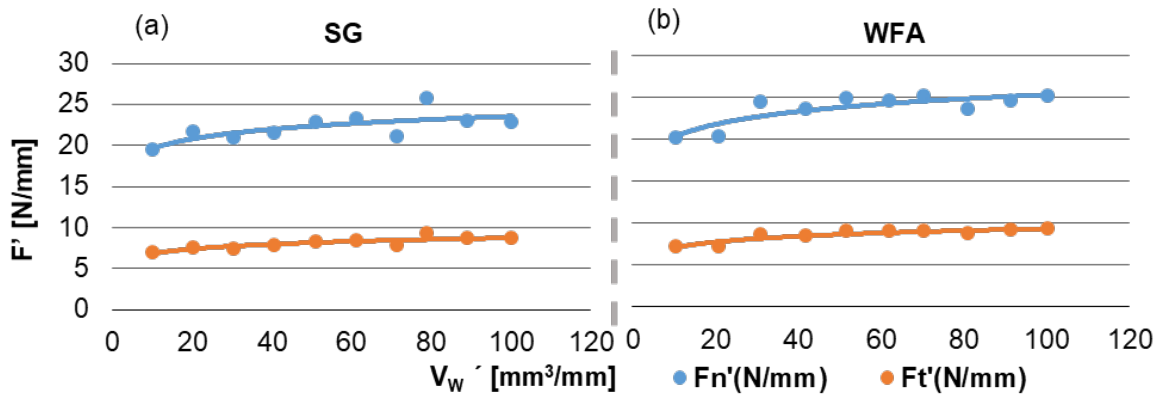

Figure 4: Normal and tangential force evolution with specific removal rate on Test 2. (a) SG alumina (b) WFA

"In spite of the different values of *%A* found between SG and WFA and the increasing tendency to observe wear flat, grinding forces present very similar values for both types of crystalline structures and increase very slightly increase, showing a quasi-constant increase. This observation is primarily due to the initial wheel surface, along with the small depth of cut achieved.

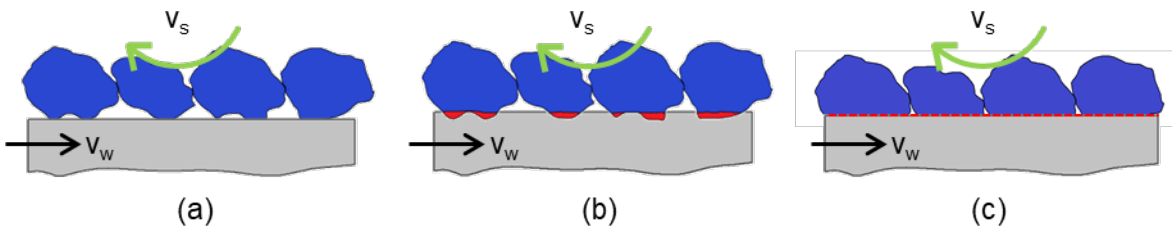

Figure 5: Contact evolution between wheel and workpiece. (a) Represent the initial contact just after dressing, (b) Representation of abrasive grain wear at the beginning of contact, (c) Representation of grinding wheel wear at the end of testing.

Figure 5 (a) represents the 1st state, the initial contact between abrasive grains and work piece. This surface has been just dressed and so the grains are sharp and represent the smallest contact area. In Figure 5 (b) the 2nd state represents grain wear for the first grinding passes. This state is rapidly achieved and the sharpness of abrasive grains is lost. Finally, the 3rd state represents the final phase of wear, at 100 mm^3/mm, Figure 5 (c). Grain flatness, together with the closed structure leads to a high contact area, which affects heat evacuation. This effect accounts for the high values of *%A* in the first 10 mm^3/mm and a fast increase in *%A*. In Section 3.2 the wheel surface roughness is analysed in order to better understand the surface modifications and its effect on the grinding force. Furthermore, due to the 3rd Body generation, sliding is the predominant phenomenon and therefore the forces do not increase with *%A*.

With regard to the grinding parameters, a small depth of cut was chosen to avoid grain breakage. Therefore, rubbing and ploughing are the main material removal mechanisms, whereas, the relevance of cutting is almost negligible. This also promotes the sliding

phenomena and the increase of temperature in the contact, leading to a *%A* increase, and again, due to the absence of the cutting mechanism the value of the grinding force is quasi-constant."

To complete the grinding analysis, the friction coefficient of Test 2 is plotted in Figure 6. Friction coefficient grows slightly with specific removal material, and hence with an increase of wear flat, ranging from 0.32 to 0.38 on both types of abrasive grains during the course of a complete test. These values of friction coefficient are in accord with results obtained from the pin on disk tribometer test used to study the wear of SG alumina [17]. Malkin also confirmed that as the hardness of the grinding wheel increases, the friction coefficient decreases in experiments carried out with wheel grade R. Quasi-constant values of friction coefficient are due to the adherence of third body to flat grains, which behaves as a metal-metal contact as opposed to ceramic metal-contact. A low value of 1.25 $mm^3/mm\ s$ is achieved during this test, and according to [6], a low specific removal rate and quasi-constant values of friction coefficient support the notion that rubbing and ploughing are predominant during these grinding tests.

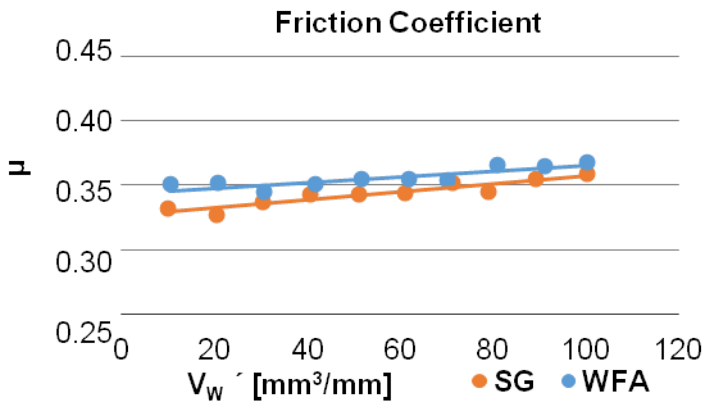

Figure 6: Friction coefficient evolution with specific removal rate for SG and WFA

The differences in % A reached on both grinding wheels together with similar values reached on force and friction coefficient prompted the microscopic study of the wheel surface in order to confirm the differences found on % A values for both type of alumina."

To sum up, *%A* increases with specific removal material but the grinding force is maintained quasi-constant for both crystalline structures. This phenomenon is due to the initial wheel surface, along with the grinding parameters designed to promote wear flat. A flat surface is achieved in the first 10 mm^3/mm. Additionally, the *%A* reached in SG alumina is higher than that for WFA. This is confirmed by the differences in thermal conductivity, in which higher temperatures were reached in the case of SG, promoting wear flat appearance. To clarify these differences, a microscopic study of the grinding wheel surface was carried out.

3.2. Microscopic analysis of wheel surface

As suggested in the previous section, a deeper analysis of the wheel surface is needed. With regard to wear flat areas, considerable differences were found in *%A* evolution and

maximum values with specific removal rate. However, no appreciable differences were found for either grinding forces or the friction coefficient. Therefore, a wheel surface analysis is required to investigate tribochemical phenomena occurring on the wheel surface during grinding.

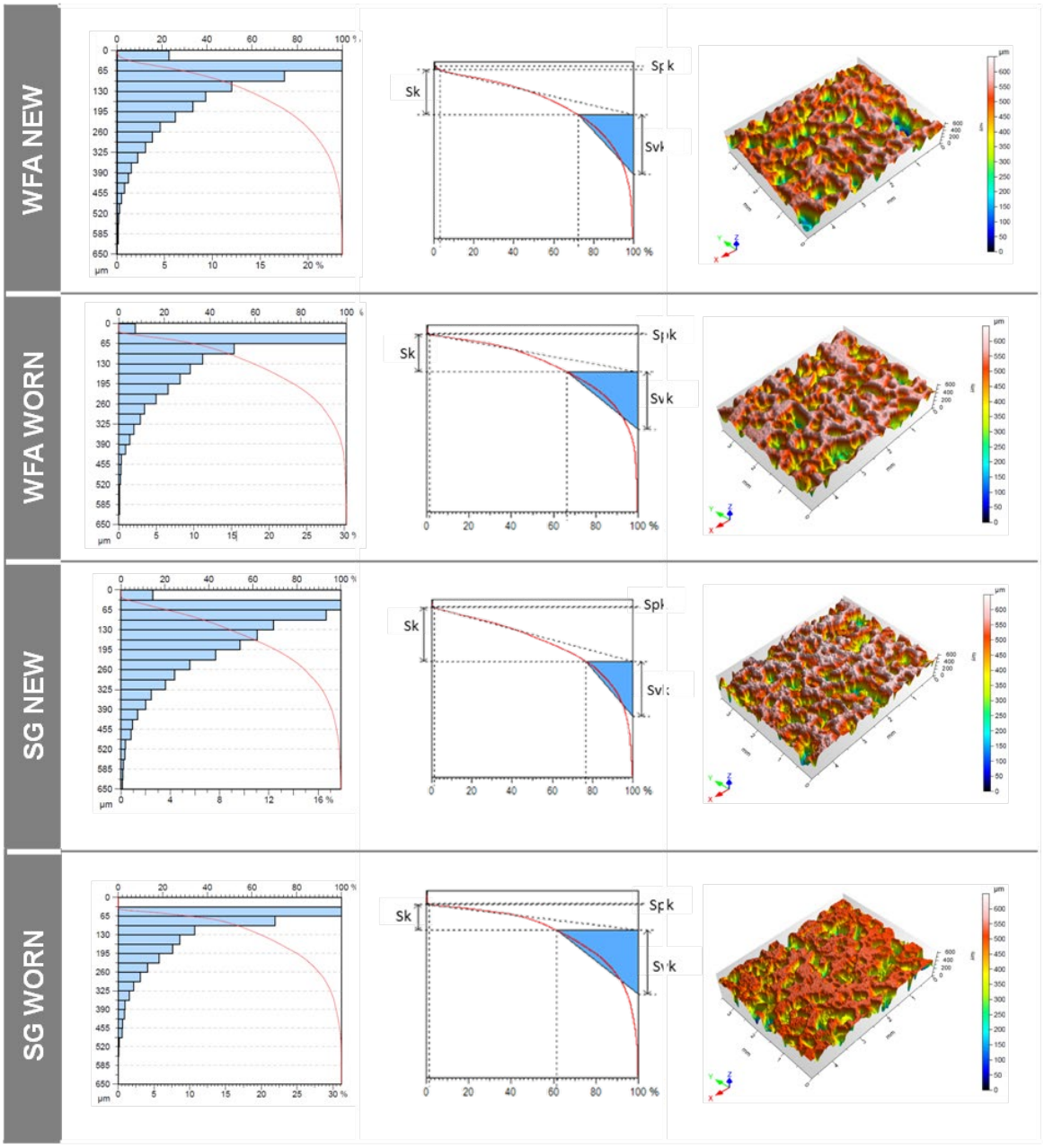

Figure 7: Functional 3D roughness parameters study for WFA and SG alumina on new and worn surfaces

Firstly, a functional roughness parameters analysis was carried out using a 3D confocal microscopy with resolution on a height of 2 µm. The dimensions of the studied surface are 3.6 x 4.75 mm^2. Figure 7 shows the 3D topography, and Abbott-Firestone curve with S_k parameters of new and worn surface for SG and WFA. Focusing attention on 3D surface

representation, SG alumina clearly presents a greater degree of wear than WFA, since the worn SG appearance is smoother than worn WFA. Additionally, analyzing loose material using the Abbott-Firestone curve, it is confirmed that only attritious wear occurs, since the depth of wear in both cases is approximately 30 µm, and the abrasive grain diameter is 250 µm.

.

Table 4: Main functional roughness parameters

	New WFA	Worn WFA	New SG	Worn SG
S_{pk} [µm]	10.8	2.13	3.7	3.11
S_k [µm]	155	125	195	79.8
S_{vk} [µm]	205	192	200	202

In Table 4 the values of the main functional roughness parameters for studying surface changes are included. S_{pk} refers to surface peaks that are above the core roughness depth. The variations in reduced peak height between 2.13 and 10.8 µm are negligible in comparison with a measurement range of 650 µm, and on first contact, these peaks are removed. The value of removed peaks is not sufficiently large to confirm volumetric wear on the wheels. In contrast, the S_{vk} value does not present changes with either crystalline structure or after wear, and thus dull material does not remain on deep holds. Therefore, S_{pk} and S_{vk} are not useful for comparing wheel wear.

In contrast, S_k is the parameter that shows the greatest variation. For WFA, S_k decreases by 30 µm with wear flat while for SG the decrease is 115.2 µm, indicating greater wear for SG than for WFA. In the Abbott-Firestone curve for SG wear the absence of material in the first 32.5 µm together with the 3D topography confirms the wear flat of SG alumina. However, it necessary to point out that the S_k parameter is not a quantitative parameter. If the distribution of the material changes, the value of S_k also changes, but the differences between new and worn surfaces are shown through core roughness depth. This parameter confirms the *%A* measured using an optical microscope and the flatness revealed on SEM images. With this measurement technique it is not be possible to distinguish between abrasive grains and dullness. Therefore, a deeper analysis is required to draw firmer conclusions and to understand tribochemical phenomena.

Figure 8 shows the analysis of wheel topography with a magnification of 50x, with an analysed area of 1.83 x 2.26 mm^2. For the new surface, WFA presents a less uniform surface than SG and different layers could be observed. Despite this difference, the starting wheel surfaces are considered sufficiently comparable for analysing the evolution of *%A*.

Once the tests had been conducted, Figure 8 (c-d) clearly shows the wear of abrasive grains, revealing the differences between the WFA and SG surface. At a magnification of 50x, the topography of SG represents a more continuous and homogeneous surface than the WFA wheel. In addition, the grinding direction can be observed in Figure 8 (d), from left to right in the image. Although the WFA surface is flat, it is possible to distinguish abrasive grains, but this is not the case for the SG wheel. The areas of worn surfaces are highlighted in green in Figure 8 (e-f), representing the flat parts of the surface after a complete test. The areas on

the SG alumina are larger than those of the WFA and almost all areas on the SG wheel are connected, unlike the case of WFA.

Further analysis was conducted with a magnification of 500x on Figure 9, in which the analysed surface is of 183 x 226 μm^2, allowing for a detailed analysis of one abrasive grain. These images verified grain flatness after grinding. The grain surface before and after the tests was also compared taking into account roughness of flat grains, since this is one of the parameters that influences third body adhesion.

Figure 9 (c-d) shows in detail the worn grains. Both WFA and SG show the flat face of the grain. In the case of WFA the grain contact face changes in appearance when it is worn (see Figure 9 (c)) in comparison with the new grain surface (see Figure 9 (a)). In this image, the surface presents white particles that have been analysed by EDXA, These are diamond particles that result from the initial grinding wheel dressing. These particles do not affect the tests. Under these particles the smooth surface is shown, making the adhesion of third body difficult. However, the worn grain surface is changed to a rougher surface, as can bee seen in Figure 9 (c).

In contrast, SG abrasive grains present the same surface on both new and worn grains (Figure 9 (b-d). This is due to the microcrystals that characterize the SG grain surface. The SG grain surface promotes third body adhesion more than worn WFA, and the roughness of SG is always constant, and is the highest of the studied wheel surfaces.

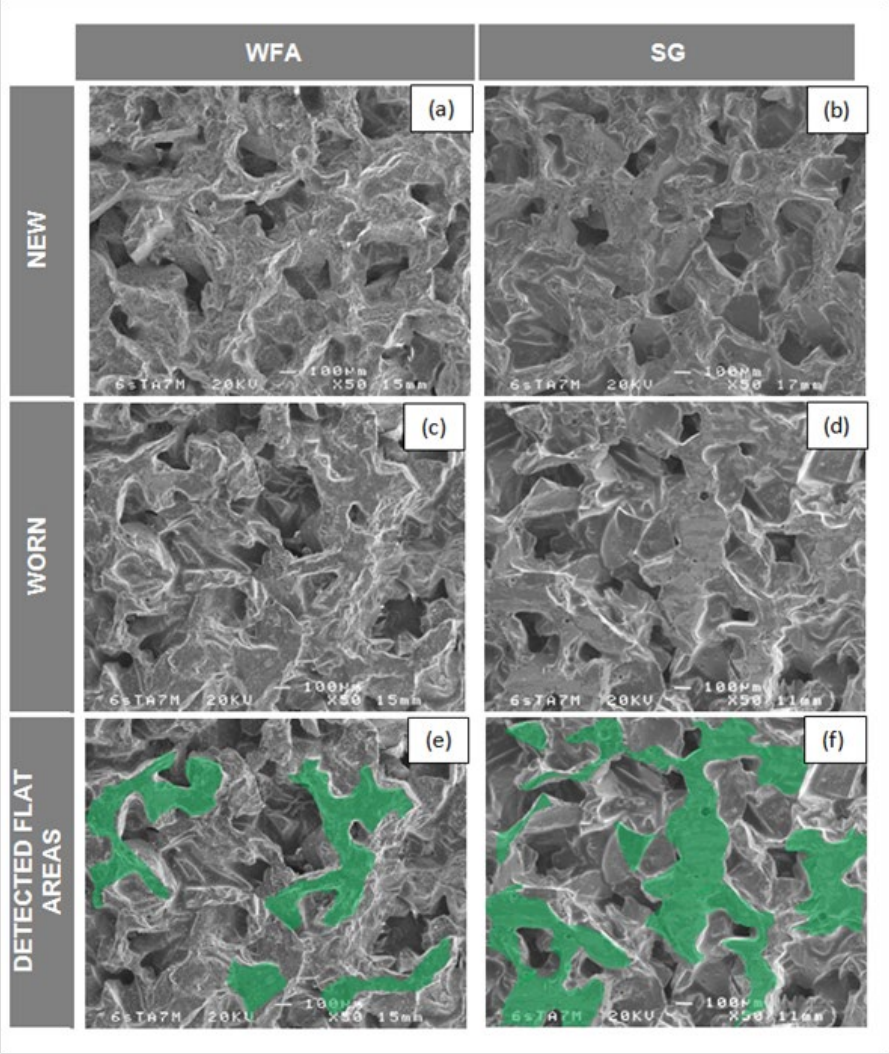

Figure 8: SEM images taken at a magnification of 50x for WFA and SG alumina on new and worn surfaces.

Accordingly, the appearance of third body adhesion to the flat grains can be observed after the tests on both crystalline structures, Figure 9 (c-d), but in a greater quantity in the case of the SG surface, as also shown in Figure 8 (e-f). This difference is largely due to the discrepancies in the temperature reached, and the characteristic of flat surfaces provided by the crystalline structure of alumina. High temperatures accelerate chemical reactions, which generate a higher quantity of third body. Furthermore, the roughness of the SG abrasive grains promotes the adhesion of the third body to flat surfaces, causing it to remain on the grains.

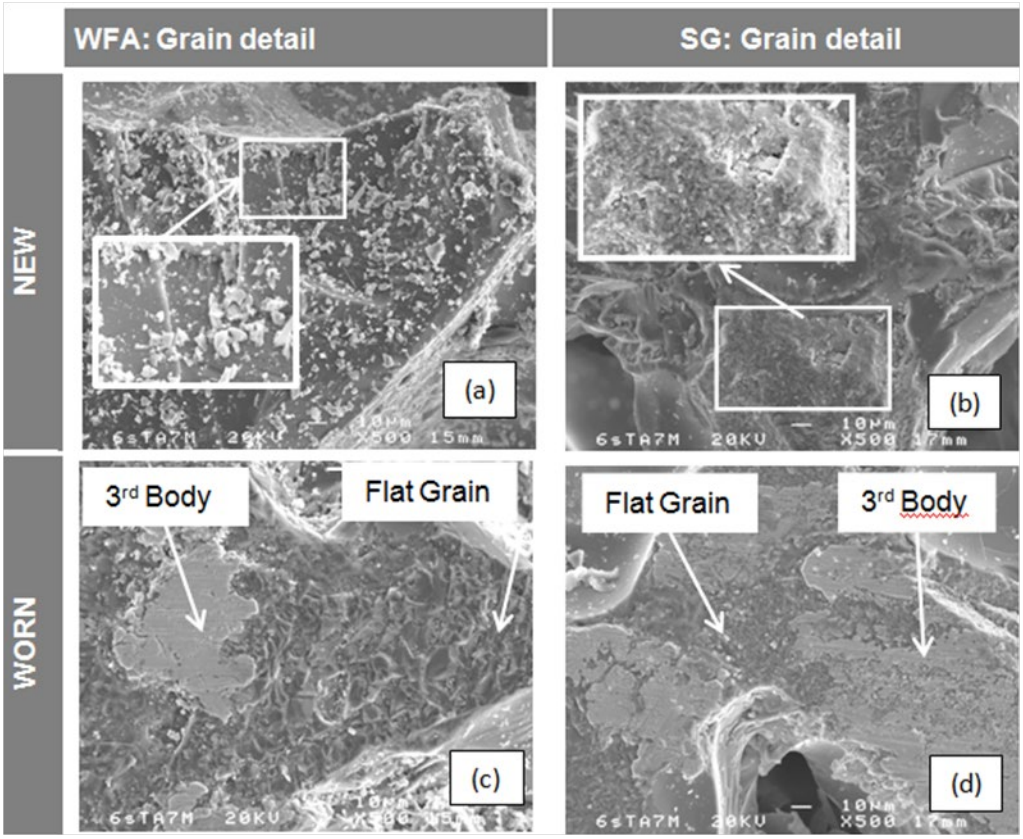

Figure 9: SEM images taken at a magnification of 500x for WFA and SG alumina on new and worn surfaces.

In Figure 9 (c-d), the third body is easily identified on worn surfaces. Its appearance in both cases is the same, with a flat irregular shape. The third body changes the contact conditions, becoming increasingly important in the case of contact between steel and third body in comparison with steel and alumina contact. The scratch marks due to friction demonstrate that the third body is in contact with the workpiece, keeping friction coefficient at a quasi-constant value of around 0.35. This quantity of third body is obtained due to the fact that during the test there is a lack of grain loss, and hence third body loss.

To continue studying the third body, an EDXA analysis was carried out. The same four zones can be identified on both WFA and SG. In Figure 10 the four zones are highlighted, while in Figure 11 EDXA graphs are plotted with the elements found.

Zone A corresponds to a vitreous bond, with Si being the main element. Zone B is the abrasive grain, and thus Al is the principal element, whilst Zones C and D refer to the third body. Third body is generated due to chemical reactions and abrasion between abrasive grains and the workpiece. In addition to workpiece material, contact conditions also exert an influence on third body composition. Iron oxides are predominant in Zone C, which is represented as a very white color on Figure 10 due to the presence of Fe and Cr. However, Zone D is recognized on Figure 10 with a grey color due to the presence of Al in addition to Fe. Iron spinels are identified in this zone. The results obtained by Klocke on pin on disk tribometer studying sol gel sintered alumina against steel disk [16] could be applied to the grinding tests employed in the present work. It is possible to affirm that Zone D corresponds

to thinner layers that are only attached to abrasive grains, whilst Zone C corresponds to thicker layers that generally cover the spinel.

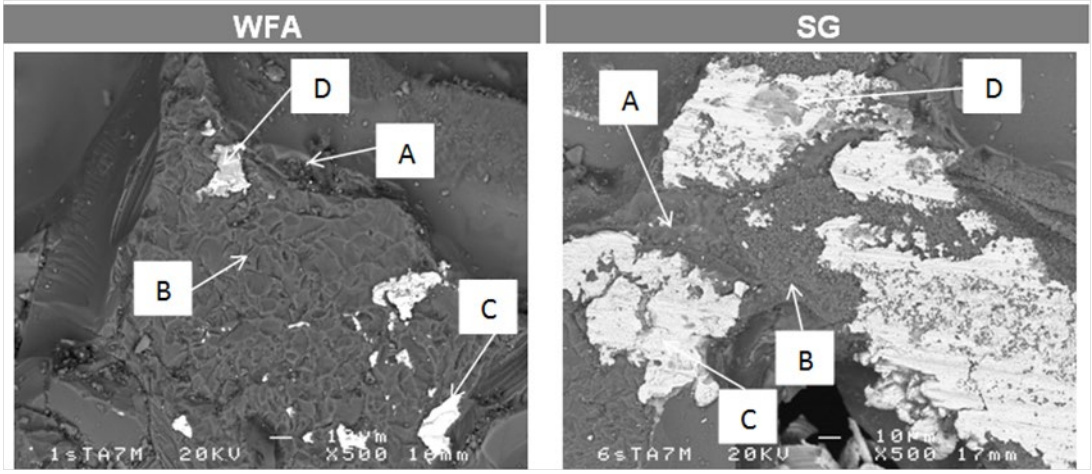

Figure 10:Identification of evaluated zones on worn WFA and SG wheels. Zone A, bond; Zone B, abrasive; Zones C and D, third body.

During the current experimental work, the measured wear flat area not only corresponds to abrasive grains but also to bond. The high temperatures reached on contact remain on abrasive grains as well as on the bond. In both cases, abrasive grains are in a vitreous bond environment, and thus the temperature reached for abrasive grains is conducted from grains to bond. However, as previously mentioned, the SG wheel reaches a higher temperature than the WFA and thus the bond evolving SG grains heat up more than in the case of WFA wheels.

The fusion temperature of silica is lower than that of alumina. The melting of the bond occurs at temperatures of around 1200ºC [22], while SG abrasive grains are melted at around 2000ºC. The temperature reached on contact is not measured in the current experimental work, but the literature reports values in excess of approximately 1300ºC [23]. The bond of the SG wheels is modified due to the high temperature and the contact with the workpiece. In habitual grinding, the bond is lost with abrasive grains, but in this case, due to wheel hardness (R) this loss does not occur, so, the third body remains on both the abrasive grains and the modified bond.

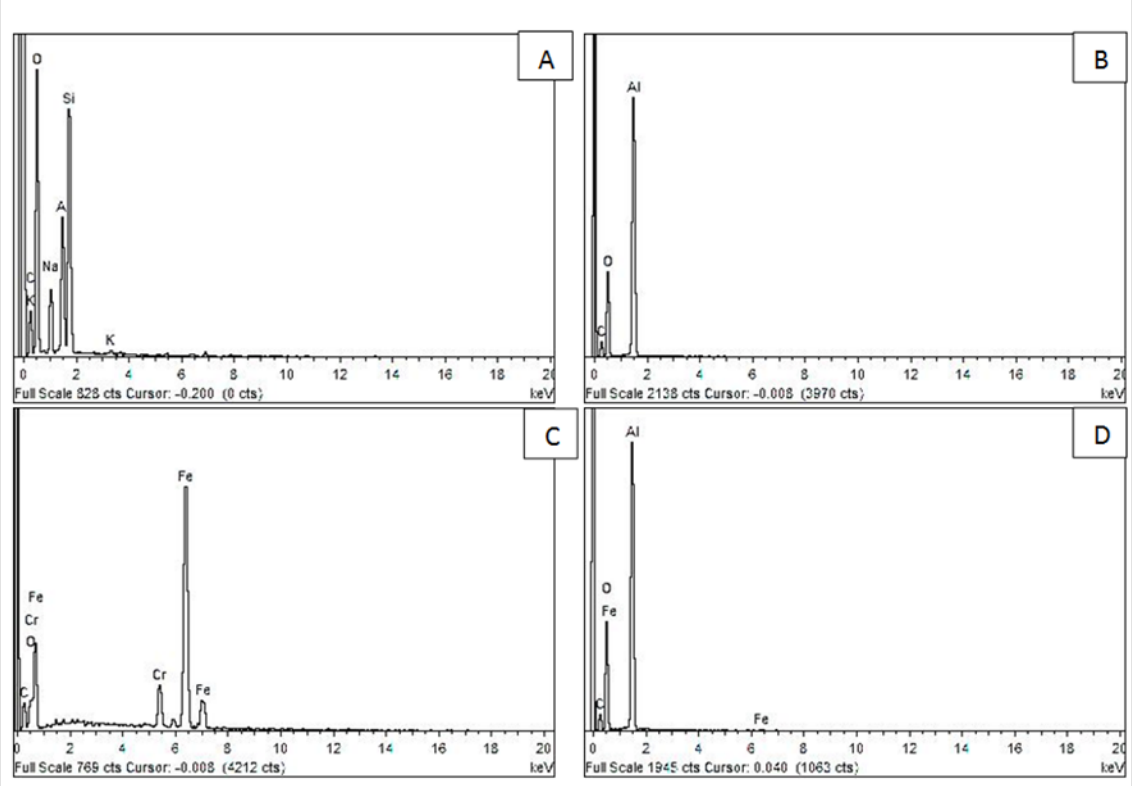

Figure 11: EDXA analysis of SG alumina for 4 different zones.

These facts explain why the appearance of worn SG wheel is more homogenous and continuous than worn WFA. This also accounts for the maximum values of 14 % of wear flat observed during experimental work on the SG wheels. The value of *%A* measured is not affected by bond modification, since light reflection occurs on flat abrasive grains and the third body, but not on the bond (whether raw or modified) due to its transparent color. Moreover, the similarities found between both types of wheels in terms of forces and friction coefficient are due to the initial surface designed to promote wear flat, along with the grinding parameters. Grinding wheels are without cutting ability almost from the beginning of the test. The sharpness presented on the SG wheel is quickly lost and the flatness and third body leads to a quasi-constant force.

4. CONCLUSIONS

The present study examined the evolution of wear flat in alumina grinding wheels by isolating and promoting this effect. The analysis was conducted on both WFA and SG wheels, and a comparison of wear flat evolution was made between both crystalline structures. Although there were few discernable differences in the behavior of each structure, there was a notable influence of the crystalline structure on both the appearance of the grinding wheel surface and on the *%A* reached, both of which were more strongly affected than the grinding parameters. Following a discussion of these results, the following conclusions can be drawn:

- Wear flat presents a linear increase both for WFA and SG alumina, with a similar slope observed in both cases. These results are broadly consistent with the results obtained by Malkin [12] and they appear to point to the possibility that the pattern of wear flat growth depends mainly on the grinding parameters.
- In the case of SG grains, the value of the total wear flat area is around 23% higher than that of WFA grains. These results confirm the influence of the crystallographic structure on the appearance of wear flat, and quantify this effect for SG grains."
- With regard to grinding parameters, workpiece speed has more influence on wear flat development than on *%A* value. The pattern of wear flat development presents a higher slope for higher v_w, whilst *%A* increases with a depth of cut between 2 and 5 μm.
- The maximum *%A* reached is of 14 % for SG alumina at v_w=15000mm/min and a_e=5 μm after 100 mm^3/mm of workpiece material removed.
- Both tangential and normal force-directions remain constant independently of depth of cut and crystalline structure. The same pattern of results is also found for the friction coefficient. This phenomenon is due to the initial wheel surface, along with the grinding parameters designed to promote wear flat, ensuring that sliding is the main phenomenon that occurs during grinding.
- 3D roughness analysis revealed differences between new WFA and SG, with the SG surface being sharper than WFA. However, after testing, the SG surface was found to be flatter than WFA. SG accumulates 32.5 % of material from 32.5 μm to 65 μm, while WFA accumulates the same quantity of material in the first 65 μm.
- Analysis of the grinding wheel surface revealed differences on just dressed and worn topography. For worn surfaces at a magnification of 50x, SG presented a smoother appearance than WFA. However, at a magnification of 500x the microcrystals of the SG wheel are noticeable, leading to a rougher surface and promoting third body adhesion.
- Once the tests had been completed, it was found that SG presented a very homogenous appearance with a higher quantity of third body attached in comparison with WFA. Both phenomena are due to the fact that the thermal conductivity is lower in SG and hence the temperature is higher on contact, accelerating chemical reactions and modifying the bond on contact. Third body adheres to both flat abrasive grains and the transformed bond.
- Finally, this work has demonstrated that in conditions where the most important material removal mechanisms are ploughing and rubbing (e.g. finishing operations), the main problem of SG grains when compared with the WFA grains is the excessive wear flat generated during the process. As the presented analyses show, the reason for this behavior is the crystallographic structure of the abrasive grain. This idea is in accord with what is found in industrial practice and will help wheel manufacturers to better understand the grinding process and to base their selection of abrasive grains not only on experience but also on scientific knowledge.

5. ACKNOWLEDGEMENTS

The authors gratefully acknowledge the funding support they received from the contracting call for the training of research staff in UPV / EHU 2016, of Vice-rectorate of research to develop this research project. And also wish to thank the Spanish Ministry of Economy for their support for the Research Project: 'Optimization of finishing processes for critical components of jet engines' (DPI2014-56137-C2-1-R).

6. REFERENCES

[1] W. Liu, Z. Deng, Y. Shang, and L. Wan, "Effects of grinding parameters on surface quality in silicon nitride grinding," *Ceram. Int.*, vol. 43, no. 1, pp. 1571–1577, 2017.

[2] M. K. Sinha, D. Setti, S. Ghosh, and P. V. Rao, "An investigation on surface burn during grinding of Inconel 718," *J. Manuf. Process.*, vol. 21, pp. 124–133, 2016.

[3] Y. B. Tian, F. Liu, Y. Wang, and H. Wu, "Development of portable power monitoring system and grinding analytical tool," *J. Manuf. Process.*, vol. 27, pp. 188–197, 2017.

[4] K. Nadolny, "State of the art in production, properties and applications of the microcrystalline sintered corundum abrasive grains," *Int. J. Adv. Manuf. Technol.*, vol. 74, no. 9–12, pp. 1445–1457, 2014.

[5] I. D. Marinescu, M. Hitchiner, and E. Uhlmann, *Handbook of machining with grinding wheels*. 2006.

[6] W. B. Rowe, "Principles of Modern Grinding Technology," in *Elsevier*, 2009, pp. 40–42, 82–87.

[7] K. Nadolny, "Wear phenomena of grinding wheels with sol – gel alumina abrasive grains and glass – ceramic vitrified bond during internal cylindrical traverse grinding of 100Cr6 steel," *Int. J. Adv. Manuf. Technol.*, vol. 77, pp. 83–98, 2015.

[8] G. Li, S. Yi, S. Sun, and S. Ding, "Wear mechanisms and performance of abrasively ground polycrystalline diamond tools of different diamond grains in machining titanium alloy," *J. Manuf. Process.*, vol. 29, pp. 320–331, 2017.

[9] I. Pombo, X. Cearsolo, J. A. Sánchez, and I. Cabanes, "Experimental and numerical analysis of thermal phenomena in the wear of single point diamond dressing tools," *J. Manuf. Process.*, vol. 27, pp. 145–157, 2017.

[10] S. Malkin and C. Guo, "Grinding technology. Theory and Applications of machining with abrasives," 2008, pp. 100–200.

[11] S. Malkin and N. H. Cook, "The wear of grinding wheels. Part 1: Attritious wear," *J. Eng. Ind.*, pp. 1120–1128, 1971.

[12] S. Malkin, "The wear of grinding wheels. Part2: Fracture wear," *J. Eng. Ind.*, pp. 1129–1133, 1971.

[13] A. Ravikiran and S. Jahanmir, "Effect of contact pressure and load on wear of alumina," *Wear*, vol. 251, no. 1–12, pp. 980–984, 2001.

[14] A. Ravikiran and B. N. Pramila Bai, "High Speed sliding of Al2O3 pins against an En-24 steel disc," vol. 13, no. 2. pp. 296–304, 1993.

[15] A. Ravikiran, G. R. Subbanna, and B. N. Pramila Bai, "Effect of interface layers formed during dry sliding of zirconia toughened alumina (ZTA) and monolithic alumina against steel," *Wear*, vol. 192, no. 1–2, pp. 56–65, 1996.

[16] J. Mayer, R. Engelhorn, R. Bot, T. Weirich, C. Herwartz, and F. Klocke, “Wear characteristics of second-phase-reinforced sol-gel corundum abrasives,” *Acta Mater.*, vol. 54, no. 13, pp. 3605–3615, 2006.

[17] S. Kannappan and S. Malkin, “Effects of Grain Size and Operating Parameters on the Mechanics of Grinding,” *Journal of Engineering for Industry*, vol. 94, no. 3. p. 833, 1972.

[18] T. M. Besmann, N. S. Kulkarni, J. D. Vienna, and K. E. Spear, “Predicting phase equilibria of spinel-forming constituents in waste glass systems,” *Ceram. Trans.*, vol. 168, no. c, pp. 121–131, 2005.

[19] S. Lachance, R. Bauer, and A. Warkentin, “Application of region growing method to evaluate the surface condition of grinding wheels,” *Int. J. Mach. Tools Manuf.*, vol. 44, no. 7–8, pp. 823–829, 2004.

[20] J. F. G. Oliveira, R. T. Coelho, and C. K. Neto, “Development of an Optical Scanner To Study Wear on the Working Surface of Grinding Wheels,” *Mach. Sci. Technol.*, vol. 3, no. 2, pp. 239–253, 1999.

[21] F. Klocke, R. Engelhorn, J. Mayer, and T. Weirich, “Micro-Analysis of the Contact Zone of Tribologically Loaded Second-Phase Reinforced Sol-Gel-Abrasives,” *CIRP Ann. - Manuf. Technol.*, vol. 51, no. 1, pp. 245–250, 2002.

[22] D. Herman and J. Markul, “Influence of microstructures of binder and abrasive grain on selected operational properties of ceramic grinding wheels made of alumina,” *Int. J. Mach. tools Manuf.*, vol. 44, pp. 511–522, 2004.

[23] S. Malkin and C. Guo, “Thermal Analysis of Grinding,” *CIRP Ann. - Manuf. Technol.*, vol. 56, no. 2, pp. 760–782, 2007.